Award G16AP00096

Collaborative Study: The 2016 East Bay Seismic Investigation of the East Bay Plain and Oakland Hills

Luther M. Strayer[1], Rufus Catchings[2],
Joanne Chan[2], Ian Richardson[1], Adrian McEvilly[1],
Mark Goldman[2], Coyn Criley[2], Robert Sickler[2]

[1]*Department of Earth & Environmental Sciences, California State University, East Bay,*
[2]*Earthquake Science Center, United States Geological Survey*
luther.strayer@csueastbay.edu, catching@usgs.gov, jchan@usgs.gov, ian.richardson@csueastbay.edu,
adrian.mcevilly@csueastbay.edu, goldman@usgs.gov, ccriley@usgs.gov, rsickler@usgs.gov

ABSTRACT

The active trace of the Hayward Fault (HF) near San Leandro, California defines the core of the Hayward Fault zone (HFZ), which is one of the major seismic hazards in the San Francisco Bay Area. The Quaternary-active, strike-slip, Chabot Fault (CF) lies ~2 km east of and parallel to the active HF trace. The HF and CF appear to bound the San Leandro block (SLB), a massive, 25 km-long Jurassic gabbro; the majority of HFZ seismicity is thought to occur near the western edge of the SLB. Piercing-point evidence suggests that ~15% of total slip on the HFZ was accommodated by the CF. Relative to the active trace of the HF that records ~5 km of slip, the CF likely has somewhere between 25-50 km of slip (Graymer et al. 1985). In its earlier role, it may have served as the active trace of the HFZ. The SLB is likely the root zone of a swath of intense reverse and strike-slip deformation that forms an 8- to 12-km-wide 'flower-structure' in the near surface. This deformation is clearly visible in the East Bay hills and likely extends beneath the sediments of the East Bay plain. If the 2014 West Napa earthquake is an indicator, subsidiary faults, such as the Chabot Fault, Redwood Canyon Thrust (our name), Miller Creek Fault, Ashland Thrust, and other mapped, suspected, and unnamed faults, should be the focus of renewed investigation. In response to this potential hazard, we conducted the 2016 East Bay Seismic Investigation (EBSI-16) during the Fall of 2016, which was a NEHRP (G16AP00096, Strayer) collaborative effort between the United States Geological Survey (USGS) and the California State University, East Bay (CSUEB) that directly followed the 2016 Napa Seismic Investigation (NSI-16), which also involved USGS and CSUEB personnel. We leveraged the cooperation between the two projects and PIs to benefit planning and logistics of both projects. We recognized a special opportunity to increase the size and scope of the originally proposed EBSI-16 study to a scale similar to NSI-16 (~20 km-long arrays). Thus, the EBSI-16 investigation became a 15-km-long survey across the greater HFZ, extending from the San Francisco Bay shoreline in San Leandro, California to nearly San Ramon, California. The EBSI-16 deployment consisted of (1) a 15-km-long linear seismic profile, normal to the HFZ. Along the profile, we used a total of 296 seismographs, with 142 two-component (P- and S-wave) seismographs spaced at 100-m intervals along the entire array and 154 vertical-component seismographs

spaced at 20-m intervals across mapped or suspected faults. We used Reftek RT-125 seismographs with 40-Hz P-wave and 4.5-Hz 3-component sensors. All data were acquired using active-source, down-hole explosions or 226-kg accelerated weight-drops where drilling was not permitted. A total of 26 shot points were used, with 16 shot points along the linear array, spaced at ~1-km intervals, and 10 off-line shots, located within major faults of the HFZ so that guided waves would be generated. The resulting data volume is large and is of high quality. The increased scope of EBSI-16 was not matched by increased project funding. Increased equipment and supply volumes and contractor costs expended our budget at the completion of field work. In the time since, we have made only partial investigations into data quality and produced only preliminary models that are, nonetheless, quite compelling.

TABLE OF CONTENTS

LIST OF FIGURES

1.0 INTRODUCTION

The Hayward Fault (HF) is one of the major seismic hazards in the San Francisco Bay Area (WGCEP/UCERF 2013), and in particular, in the East Bay, where the fault dominates the topographic grain of the region, as well as the distribution of housing, industry, and infrastructure adjacent to the fault. The predicted strong ground motion from a characteristic HF event (M 7.0+) will affect the region, the State, and the Nation, due to economic and human losses (Maffei et al., 2010).

The greater Hayward Fault zone (HFZ) is a minimum of 8 km wide as mapped, without considering possible connecting faults that would likely be obscured beneath the sediments of the East Bay plain. In the San Leandro area, the wider HFZ has multiple significant splays that trend subparallel to the main active trace (Fig. 1). In the region between San Leandro and Hayward, the core of the HFZ is composed of a fault-bounded, ~2-3-km-wide, lithotectonic block, composed of Jurassic mafic intrusives (mainly gabbro) and mixed-composition volcanics, that is ~25 km long. This San Leandro block (SLB) is bounded on its west side by the active trace of the Hayward Fault (HF). On its east side, the Quaternary-active Chabot Fault (CF) juxtaposes Jurassic igneous units against Cretaceous clastic rocks (Graymer, 2000). The SLB is effectively a horst, described as a steeply eastward dipping tabular mass with a broadly rectangular shape that extends to at least 6 km depth, as inferred by gravity and magnetic studies (Ponce et al., 2004). At its margins, the fault core/SLB appears to serve as the steepening root zone for both east- and west-verging subsidiary reverse faults, such as the east-dipping Piedmont (Trench et al., 2015) and Ashland reverse faults and the west-dipping thrusts in the East Bay hills (Graymer, 2000).

This system of strike-slip and reverse faults progressively juxtaposes older and originally deeper Jurassic igneous units against Cretaceous units, which in turn are thrust over Tertiary and possibly Quaternary materials, as with the Piedmont thrust. The faulting pattern infers a flower structure that appears to root into the core zone. The subsidiary reverse faults likely play an important role in the partitioning of compressive strain in the shallower levels of the fault zone, where shortening across the fault is accommodated by folding and faulting. There is a gross pattern of relative parallelism of long portions of the flower structure thrusts to the strike of the HFZ. This suggests that, at least to the depths where the reverse faults merge/root into the main fault zone, the core of the fault zone may be relatively weak compared to deeper parts of the fault (Mount & Suppe, 1987). This is a familiar structural style associated with strike-slip faults that effectively partitions upper-level, transpressive motion between the central strike-slip and the outward-splaying reverse-slip faults, whose slip directions are normal to the trace of the main strike-slip system (Fossen, 2010, p.363).

The Hayward and Chabot faults (do you want to use upper or lower case? Earlier you used upper case for Chabot Fault.) have nearly identical orientations. Geologic mapping shows the two faults to be subparallel for at least 25 km and are separated by only ~2-3 km (Graymer, 2000; Lienkaemper, 2008) of severely deformed gabbroic rock in many locations. Mohr-Coulomb (M-C) theory predicts that two similarly oriented faults like the Hayward and Chabot faults are equally likely to fail if the strengths of both are the same. Byerlee's (1978) law, combined with M-C theory, predicts faults in upper crustal rocks at modest depths and confining pressures, regardless of lithology, will likely have similar strengths. The CF is, therefore, in an ideal orientation to accommodate excess slip that might shed from the Hayward Fault during a large earthquake. Sympathetic slip on the CF, in response to a large Hayward Fault event, may

well be transferred to the west-dipping, east-verging reverse faults that must merge with the CF at depth. The recent example of the 2014 South Napa earthquake, which involved seemingly less active strands of the West Napa Fault, illustrates the hazard posed by similarly oriented faults that have effectively similar strength characteristics. This situation resulted in unexpected ground rupture and damage outside the established Alquist-Priolo zone. It is, therefore, important that we re-evaluate important subsidiary faults with apparently favorable orientations for reactivation and potential for slip.

For the 2016 field season, we proposed a modest, cooperative (CSUEB-USGS) seismic imaging study across the HFZ that was funded by NEHRP (G16AP00096) and which ultimately became the 2016 East Bay Seismic Investigation (EBSI-16, PI Strayer, Co-PI Catchings). In concert with personnel from the USGS Earthquake Science Center, Bay Area students, and community volunteers, we completed EBSI-16 in October 2016, directly following completion of the Napa Seismic Investigation (NSI-16, PI Catchings, Co-PI Strayer). These two studies were cooperatively planned and prepared simultaneously in the Spring and Summer of 2016 to share as much of the same equipment, personnel, and methods for both efforts.

For our original, funded NEHRP16 study, we proposed to "acquire one seismic line that will cross the SLB in the area around Castro Valley." We deliberately made the details of length and resolution for the proposed array vague, simply because the nature and potential extent of our access to both public and private lands were unknown. Permitting became the most difficult and time-consuming aspect of the whole endeavor. Our degree of success in permitting, more than any other factor, would determine the depth, resolution, and quality of the resulting study.

Our realistic expectation when writing the initial proposal was that we would likely be able to acquire one or two high-resolution (3-5 m shot/sensor spacing), wired seismic lines across a slender (~1 km wide) section of the SLB, near Lake Chabot, that would allow us to image both the HF and CF that bound Fairmont ridge and some of the many intervening splays. These data would have afforded refraction (Vp, Vs), reflection, guided-wave, and multichannel analysis of surface waves (MASW) analyses. We expected it would likely illuminate important velocity structure for the SLB and allow for better locations of known faults and unknown splays between the HF and CF that bound Fairmont ridge.

We recognized during the combined planning of both the NSI-16 and EBSI-16 that we had a special opportunity to scale-up the modest HF investigation well beyond what was initially proposed. Given the clear seismic hazards and scientific importance of both (Napa and East Bay) studies, the large efforts required to secure permits and to arrange equipment and logistics, it made sense to expand the HF study to dimensions similar to those of the Napa study, where we acquired two ~20-km-long seismic arrays parallel to and across Napa Valley. Thus, we chose to acquire as much high-quality data for the Hayward study as possible, given our time and budget considerations and the number of personnel available. The result was a high-volume of high-quality data, community buy-in and involvement, and significant press coverage, including a Science Channel special focusing on the experiment and fault hazards in the San Francisco Bay Area.

The goal of this initial (NEHRP16) proposed study was to determine the fault geometry at depths above the seismogenic zone, which constitutes a data gap for fault geometry between that determined by geologic mapping and that determined by relocated seismicity. This remains the primary goal of our research and a recently submitted NEHRP (2018) proposal. However, one of the most important and time-sensitive results that we have yet to, but will derive from these data, is the shear-wave velocity structure model (Vs) across the East Bay, which currently

represents the highest resolution Vs data available across the HF area. We intend to carefully process, analyze, and disseminate the Vs data in a timely manner so that it can be rapidly included in the Bay Area 3-Dimensional (3D) Velocity model and subsequently used in strong ground-motion modeling studies. As proposed in the initial 2016 effort, we have also made progress on building detailed 3D models of the HFZ by correlating some of the initial models with recognized surface faults and projecting them to depth. From guided-wave analysis, we will gain insight into the nature and degree of fault connectivity, and ultimately, project the faults to depth into the upper seismogenic zone.

The EBSI-16 survey resulted in a wide swath of data across the East Bay plain and hills that had not previously been seismically imaged at that scale. The in-line and guided-wave shot-gathers, the MASW analysis, and the preliminary Vp- and Vs-derived tomography models are quite exciting. Initial models show that seismic velocities of the HFZ, the East Bay plain, and the East Bay hills are illuminated to depths of 5-6 km, with initial reflection analysis to depths of ~10 km. The data quality and early results from the investigation are excellent and compelling.

2.0 TECTONIC SETTING AND PREVIOUS WORK

The SLB is composed of Jurassic to Cretaceous-aged serpentinized gabbro, basalt, and minor felsic volcanics (Radbruch-Hall 1974; Graymer 2000). From map view, the SLB appears to be bound by the two primary faults of the HFZ near San Leandro, California, the active HF and the CF:

1) The active trace of the HF, which upon casual observation *appears* to define the western edge of the SLB, is instead within the SLB (in gabbro) and is well east of the contact between sediments of the East Bay plain and underlying basement, which is presumably the western SLB and outboard Franciscan lithotectonic packages. Not only does the HF not define the western extent of the SLB, but its true western extent is currently unknown. However, Ponce and others (2003) suggest that the SLB lies mostly east of the active trace of the HF, extends to at least 6 km depth, and dips steeply eastward based on potential fields modeling, except at the surface where it is demonstrably vertical, and;

2) The CF is a large eastern splay of the HF and presumed to be the parent of the current active trace of the HF. The CF is parallel to the HF for about 25 km (Fig.1), trending through the CSUEB campus, downtown Hayward, Castro Valley, Eden Hospital, and effectively under the Lake Chabot dam.

The northern and southern extents of the SLB coincide with the merger of the CF into the active trace of the HF in the Oakland hills and southern Hayward hills. At the southern end, north of Niles Canyon, the SLB terminates into the Garin graben, a pull-apart basin that, based on simple geometry, may have evolved during a finite time period when the active trace of the HF stepped westward and outboard, around, or *perhaps it even migrated through* the SLB to its current active-trace location. Prior-to and during this time, the CF may have served as the active trace of the HF. Relative to the current active trace, which records only about 5 km of slip, the CF likely accommodated somewhere between 25-50 km of slip (Graymer et al., 1985) in its earlier role as the main locus of HFZ slip. There are numerous small-scale faults within the SLB that cross the block as low-angle anastomosing structures that likely physically connect the HF and CF across the mapped extent of the SLB (Graymer, 2000). We believe we have identified a number of these near-vertical strike-slip faults using MASW analysis (Fig. 7b) (Richardson et al., 2016; Strayer et al., 2016) of data acquired within the SLB portion of a 15-km-long seismic profile that we completed this past Fall across the East Bay plain, the SLB, and the East Bay hills (EBSI-16).

There is a strong pattern of relative parallelism of long portions of reverse and thrust faults that are adjacent to the strike-slip-dominated core of the HFZ. It appears that the SLB may be the root zone for this 8- to12-km-wide, sub-parallel swath of intense faulting, which is clearly visible in the adjacent East Bay hills and that likely extends hidden beneath the sediments of the East Bay plain. We appear to have imaged some of this faulting in the initial tomography derived from EBSI-16 (Fig. 5).

These important subsidiary faults include the Miller Creek Fault (MCF), the Redwood Canyon thrust (RCT - our working name), the Ashland Thrust, and likely a number of other faults that are obscured beneath East Bay plain sediments west of the HFZ, including a northern extension of the Silver Creek Fault. Some of these associated reverse faults may root into the HFZ at shallow depths without producing significant seismicity (i.e. 3-4 km deep), whereas other strike-slip faults are more likely to merge deeper, and thus, may be capable of generating large earthquakes. The degree and nature of connectivity between these faults that may link with the

deeper and seismogenic HFZ is important and has profound implications for the maximum magnitude and extent of ground shaking in the East Bay, whereby guided waves from a deep (>12 km) earthquake may travel to the surface, resulting in strong ground shaking adjacent to and within connected exposed faults and unknown buried faults. This scenario creates an increased risk of strong shaking above and adjacent to these physically connected subsidiary faults, and significantly widens the HFZ footprint and the resultant area affected by damaging strong shaking. These subsidiary reverse faults likely play an important role in the partitioning of compressive strain in the shallower levels of the fault zone, where shortening across the fault may be accommodated by folding and faulting. An example comes from the west-vergent Ashland Thrust in San Leandro (crossed in EBSI-16), where there is a small uplifted wedge-shaped block of SLB gabbro that is floored by a thrust fault and bound to the east by the active trace of the HF. Presumably strain partitioning of local transpressive motion on the HF forced this small 'chip' of SLB gabbro up and over the sediments of the East Bay plain, giving a rare glimpse of the lithologies that are mostly obscured by the sediments of the East Bay plain.

It has for years been widely accepted that the SLB is a generally strong rockmass (Morrow & Lockner, 2001) and that it may fundamentally control the release of seismic energy along this portion of the HF. It has also been postulated that the SLB may act as a regional-scale asperity by nature of its geometry and strength. Although poorly constrained, the 1868 Mw7.0 HF earthquake (Yu & Segall, 1996) is believed to have originated in the area of the SLB, which may act as a nucleation site of future earthquakes. However, preliminary, unpublished seismic refraction tomography models from our new seismic survey (EBSI-16) across the wider HFZ, *sensu lato*, (includes proximal, connected, and related faults), indicates that within the upper 1–3 km, the SLB is a low-velocity feature that is likely weak. It has nearly the same Vp as the adjacent Great Valley sediments to the east, with low Vs and high Vp/Vs values. From our initial analysis of the data, we believe that we can follow the SLB and its bounding faults (HF and CF) nearly vertically to at least 2-4 km depth based on velocity contrasts. They appear to extend toward and project directly into a curtain of relocated epicenters that define active faulting beneath the HFZ at depth (Fig. 6b).

This surprising result from deep (~4 km) refraction, that the SLB may not actually be as monolithic and strong as had been thought, is consistent with our field-based understanding of the extreme and penetrative nature of deformation observed in outcrops within the SLB. A weak SLB is also consistent with the closely-spaced, 2nd-order, strike-slip faults that we were able to image in the near surface (MASW) within the SLB, between the HF and CF (Fig. 7).

Significant progress by Phelps and others (2008) in developing 3-D models of the San Francisco Bay Area, based on excellent surface mapping, geophysical studies, and seismology (Graymer 2000, Ponce 2003; 2004), has enhanced our understanding of regional fault geometries, topologies, and possible connectivity. The ultimate and long-term goal of our research is to produce similar, but smaller-scale, 3D models of the fault geometry and velocity structure of the HF system and adjacent areas by employing 3D structural geology and visualization software (MoveSoftware, 2017) and by focusing on specific areas or structures of concern, such as the SLB and the adjacent East Bay plain.

3.0 GEOLOGY OF EAST BAY SEISMIC INVESTIGATION

The study area for EBSI 2016 is located in the Coast Ranges Geomorphic Province of California. The Coast Ranges are characterized by a series of northwest-trending, folded and faulted mountain chains and intervening valleys. Mappable geologic surface units along the 15-km-long EBSI seismic line (Fig. 2) consist of Jurassic gabbro of the Coast Range Ophiolite (CRO), late Jurassic to late Cretaceous members of the Great Valley group, and Miocene to Pliocene members of the Mulholland Formation. Mapped Quaternary units include alluvial, fluvial, and natural levee deposits, bay mud, and artificial fill.

Although it does not crop out along our seismic line, the J/K-aged accretionary wedge of seafloor material known as the Franciscan complex is an essential piece of the East Bay tectonic puzzle. Scraped from the seafloor and thrust beneath the CRO, the Franciscan complex is considered to be the basement of the East Bay plain (EBP), as well as the underlying unit of the Great Valley complex.

What follows is a description of the geology and tectonics of our EBSI 2016 line, presented in road-log style. Kilometer zero is located at the SW end of the line in San Leandro, and kilometer 15 is located at the NE end of the line on Crow Canyon Road in an unincorporated area of Alameda County.

0.0 to 4.5 km The EBP, an area of low relief between the shore and the East Bay hills, is composed of Quaternary sedimentary deposits up to 1000 m thick that overlie basement rock of Franciscan complex. Previous seismic work by Catchings and others (2006b) shows the topography of the underlying basement rock as having significant relief: vertical elevation changes of >100 m suggest that faulting is indeed present beneath the EBP. Additionally, reflection and tomography from the same study indicate a number of near-surface fault zones present within this wide plain of Quaternary sediment, bay mud, and artificial fill.

4.5 to 7.0 km The core of the HFZ is marked by a dramatic increase in relief. Here, the surface geology, bounded by the Holocene-active Ashland Thrust to the SW and the CF to the NE, includes Jurassic gabbro of the Coast Range Ophiolite and Cretaceous Great Valley marine sedimentary deposits. The NE-dip of the structure and the lack of geomorphic evidence showing significant surface displacement SW of the Ashland Thrust may suggest that it is currently the westernmost significant component of the principal displacement zone of the HFZ.

Northeast of the CF, the geology along the EBSI line consists of Great Valley sediments (marine and marine margin shale, sandstone, and conglomerate), as well as members of the Mulholland Formation (marine and marine margin shale, sandstones, conglomerates and minor volcanics; Ham, 1952). A series of NNW-trending ridges and canyons, subparallel to the HF, develop out to the NW. Strikes recorded on units in the area, as well as geologic contacts, follow this general NNW trend as well. Localized deformation is pervasive along our line and throughout the East Bay hills, and overturned folds are not uncommon (Graymer, 2006).

7.0 to 11.5 km The surface geology consists of Cretaceous marine sediments of the CRO, bound to the SW by the CF and to the NE by the Miller Creek Fault (MCF). At km 10, the SW-dipping Redwood Canyon Thrust Fault emplaces the Oakland Conglomerate over the younger Redwood Canyon formation.

11.5 to 15.0 km NE of km 11.5, the geology is composed of Tertiary sediments and minor volcanics of the Mulholland Formation. These Miocene-Pliocene units are being thrust to the southwest beneath the Cretaceous Redwood Canyon Formation of the Great Valley group by the MCF (Ham, 1952; Graymer, 2006).

Cumulatively, the geomorphology and mapped geology, as well as previous drilling and geophysical investigations, indicate basement rocks are overlain in low relief by Quaternary sediments to the SW of the HFZ. Within and to the NE of the HFZ, elevation and relief increase, and Jurassic to Tertiary bedrock tends to be shallow or exposed. Tectonically controlled ridges and canyons, subparallel to the HFZ, extend to the NE beyond the extent of the EBSI-16 line.

4.0 APPROACH AND METHODOLOGY

To successfully collect seismic data across the HFZ, we focused our efforts on two major areas: 1) pre-survey literature/data review and field visits, obtaining permissions, logistical planning, and survey site preparation, and 2) seismic data collection, data processing, and preliminary modeling and analysis. The first part of our efforts occurred between May to September 2016, and the active seismic survey occurred during the first six days in October 2016.

4.1 Pre-Survey Preparations and Logistics

Prior to deployment of the seismic recording array, the Principal Investigators (PIs) planned possible recording and seismic source sites using Google Earth. We secured access permissions for every seismograph (>300) and shot-point (30) location. This process took up to five months, as the PI contacted government agencies, private corporations, schools, and churches that could potentially host a seismograph, in-line shot-point, and/or guided-wave shot-point. Moreover, approximately half of our seismographs were placed on individual properties, necessitating a crew of CSUEB student volunteers. Using Google Earth, we mapped addresses for potential seismograph locations. Student volunteers visited the sites, assessed accessibility and security, and secured permissions for access.

We prepared the survey line by drilling more than 30 holes for shot-points, which ranged from 9 to 40 ft in depth, prior to sensor deployment. We used two Bobcat skid-steer tractors with 6-inch auger attachments that were operated by USGS and CSUEB personnel.

Concurrent with the preparatory work, we coordinated with USGS Public Relations personnel and Bay Area media outlets to inform the East Bay community about the seismic investigation (EBSI-16). We understood from prior experience (c.f. EBSE-13, Catchings, Strayer et al., 2013) that large-scale seismic surveys require strong community buy-in to be successful. Thus, we held a press event near the East Bay Regional Parks headquarters at Lake Chabot in Castro Valley, where we drilled shot point number 9 (Fig. 1) in the midst of media coverage.

4.2 Seismic Profile

In October of 2016, we acquired high-resolution P- and S-wave seismic data along a 15-km-long, 2-D profile perpendicular to and across the mapped extent of the HFZ and SLB near San Leandro (Fig. 1). The actual location of the seismic line was revised from that initially planned in response to the increased scale of the survey. Due to access and safety concerns, there were two small gaps (< 250 m) in geophone sensor coverage along the profile: near I-580, on the west side of Cull Canyon road (Fig. 3). Additionally, there was a larger gap (~650 m) near the northeast end of the line. The overall seismic profile trends 054° and begins at the margin of the San Francisco Bay at the San Leandro shoreline. The profile then extends to the northeast, where it terminates within ~4.5 km of the Calaveras Fault. The profile crosses at least five significant mapped faults, four of which have been documented to be either Quaternary or Holocene active (c.f. Rubin, 2011; Wakabyashi, 2007; Graymer et al., 1995).

4.3 Survey Description

We requested RT-125A (Texan) seismographs and Sercel L-28 4.5-Hz, 3-component sensors from the IRIS/PASSCAL instrument center, and we deployed the array on October 1-2, 2016. Working in teams of up to thirty volunteers and USGS personnel, we deployed 438

seismographs along an ~15-km-long seismic profile from Heron Bay in San Leandro to Crow Canyon Road in Castro Valley (Fig. 1). We deployed 142 two-component seismographs/sensors (vertical and horizontal) spaced ~100 m apart along the total length of the seismic profile, and we deployed an additional 154 single-component seismographs (vertical sensors, spaced at 20-m intervals) across known or suspected faults along the profile (Fig. 1) To generate the seismic sources, we used explosive sources (1–40 lbs) in boreholes (spaced at ~1-km intervals) along the entire seismic profile. In locations where it was not feasible to use down-hole explosives, we used a 226-kg accelerated weight-drop to generate our seismic sources.

The seismographs were programmed to record for six hours per night, starting at midnight on October 3rd and on October 4th, while two teams of USGS personnel and volunteers coordinated shot times and activated all seismic sources (shots). We generated shots at 16 in-line locations, 14 of which were explosive sources and 2 of which were of repeated impacts from the accelerated weight-drop. In addition to the in-line explosive shots, we generated fault-zone guided waves from 10 off-line shots that were located 2 to 10 km from the linear recording array (Fig. 1).

4.4 Seismic Processing Methods

Fault-zone imaging with a combination of reflection methods, P- and S-wave refraction tomography, tomographic Vp/Vs modeling, and tomographic Poisson's ratio modeling has proven to be a highly effective method for identifying individual fault traces within fault zones (Catchings et al., 2009; 2013; 2014), particularly in the shallow (<500 m) subsurface. To examine the width, connectivity, and velocity structure of the HFZ, we used high-resolution Vp and Vs seismic imaging methods, described by Catchings et al. (2014), to developed initial tomographic images. We also developed initial shallow-depth Vs models using the multichannel analysis of surface waves (MASW) method. To more fully analyze these data sets, including developing Vp/Vs and Poisson's ratio models, developing wide-angle reflection images, and completing analysis of guided waves, we have applied for a 2018 NEHRP grant.

4.4.1 Seismic Refraction Imaging

Because fault zones are known to cause distinctive zones of relatively low P-wave velocities in rock (Catchings et al., 2001; 2006; 2014), we are able to identify fault zones at depth along the seismic profile. Our P-wave dataset consisted of approximately 4,736 traces (16 shots and 296 seismograph stations) along the 15-km-long seismic profile. We combined the data into individual shot gathers and filtered the data using the interactive seismic processing package known as ProMax. We measured first-arrival travel times on each P-wave shot gather and used Hole's (1992) tomographic inversion code to generate the initial P-wave velocity models. We used 1-D starting models calculated from the 16 in-line shot gathers along the seismic profile. We found that minor variations in the measured first-arrivals resulted in variable 1-D starting models. As a result, we used multiple starting models for our 2-D inversions, but all final models were similar, with less than 5 percent variation among them. For our initial data analysis, our preferred model is shown in Figure 5.

4.4.2 Multichannel Analysis of Surface Waves (MASW)

Using the MASW method, we modeled surface waves (Rayleigh waves) that were generated by our explosive shots to develop a shallow-depth, semi-2-D shear-wave velocity model of a segment of the seismic profile. The MASW method takes advantage of the dispersive

properties of surface waves to infer shear-wave velocities (Nazarian et al, 1986; Park et al., 2000; Xia et al., 2000b). Because dispersion of elastic waves is related to the properties of the medium through which it propagates, it can be used to infer shear-waves velocities in the shallow subsurface (Pujol, 2003). We use the common mid-point, cross-correlation (CMPCC) method, developed by Hayashi and Suzuki (2004) to construct phase velocity (dispersion) curves. We iteratively inverted the dispersion curves using the nonlinear, least-squares approach of surface-wave inversion software by Geometrics. Those inversions result in a series of one-dimensional models that are combined to construct a two-dimensional S-wave velocity model.

4.4.3 Vs30

Shear-wave velocities in the upper 30 m have been shown to be a useful proxy to estimate ground shaking at a given site (Borcherdt, 1970; Holzer et al., 2005). As a result of major structural damage that has occurred during earthquakes due to site amplification (ex: Loma Prieta in 1989), U.S. building codes require consideration of site amplification when estimating seismic demand on a structure (Borcherdt, 2002; Holzer, 1994). The time-averaged shear-wave velocity in the upper 30 m (Vs30) is a value representing site conditions used by building codes, calculating loss estimates, and ground motion prediction equations (Holzer et al., 2005; Wills et al., 2015). To evaluate shear-wave velocities along the seismic profiles, we performed MASW analysis on surface waves across three known faults along our seismic profile: Chabot, Redwood, and Miller Creek faults (Fig. 7b, c, d). From these shear-wave measurements, Vs30 can be calculated. Averaged Vs30 values were calculated for these three sites based on a series of one-dimensional shear-wave velocity models (Park et al., 2005).

5.0 PRELIMINARY ANALYSIS AND RESULTS

5.1 P- and S-Wave Shot Gathers

We present P- and S-wave shot gathers from shot points 6 and 11 (Figures 3 and 4); shot point 6 was located at approximately meter 5000 and shot point 11 was located at approximately meter 9500 along the profile. The main trace of the HF, located at approximately meter 5500 along the profile, is between shots 6 and 11. Each P-wave shot gather contains 296 traces, and each S-wave shot gather contains 142 traces. Gaps within the shot gathers show locations where we could not deploy seismographs due to access concerns. P- and S-wave shot gathers at shot point 6 (Figures 3 and 4) show seismic wave propagation across the length of the profile. However, P- and S-wave shot gathers at shot point 11 (Figures 3 and 4) show seismic wave propagation to the east of the HF but not to the west.

5.1.1 P-Wave Refraction Tomography

P-wave velocities ranged from less than 1000 m/s at the surface to more than 6000 m/s at depths greater than 3500 m (Fig. 5). The lowest velocities are located at the tidal marsh in the southwest, but velocities increase to the northeast toward the East Bay hills. Local areas of low P-wave velocities in the upper 100 m appear at meter 12,000 of the seismic profile, which corresponds to the mapped location of the MCF, and at meter 14,000. A high P-wave velocity structure at 1500 m depth is located just southwest of the Ashland Thrust Fault. This high P-wave velocity structure at depth coincides with the interpreted serpentinite body that Ponce et al. (2003) infer in their study.

5.1.2 MASW 2-D Shear-wave Velocity Models

We developed S-wave velocity models using the MASW method along three sections of the profile where seismographs were spaced at 20-m intervals. The depths of imaging range from 100 to 200 m. Our westernmost MASW model (Fig. 7b) crosses the Hayward and Chabot faults and is ~2 km long. Shear-wave velocities along this section of the profile range from 500 to 1600 m/s. Our central MASW model crosses the Redwood Canyon Thrust Fault (Fig. 7c) and is 960 m long. S-wave velocities across this section range from 400 to 1600 m/s. Our easternmost MASW model (Fig. 7d) crosses the MCF and is 480 m long, with S-wave velocities ranging from 400 to 1200 m/s. Low S-wave velocity zones coincide with mapped faults in these three models, with two noticeable low-velocity zones a few hundred meters east of the CF and a large low-velocity zone extending from about 300 m east of the Redwood Fault and to the end of our model.

5.1.3 Average Vs Values in the Upper 30 m (Not Time Averaged)

S-wave velocities in the upper 30 meters (Vs-average) were calculated from 1-D MASW S-wave velocities. Vs in the Hayward-Chabot section ranges from 550 to 1270 m/s with an average Vs value of 800 m/s. Vs in the Redwood Canyon Thrust Fault section ranges from 420 to 1070 m/s with an average Vs value of 753 m/s. The Miller Creek section Vs values ranges from 370 to 1260 m/s with an average Vs value of 565 m/s.

6.0 SUMMARY OF FINDINGS

Some preliminary results from the East Bay Seismic Investigation are summarized below.

- P-wave velocities at depths greater than 1 km within the San Leandro Block (SLB) are similar to those seen in the JK-aged Great Valley sediments (shale and sands) located east of- and juxtaposed across the Chabot Fault. Because the SLB is believed to be composed of gabbro, this is an unexpected finding. Significant and concentrated brittle-plastic deformation seen in the SLB throughout the study area may account for this surprising result (Fig. 5).

- At about meter 4500 of the seismic profile (west of the surface exposure of the SLB) at ~ 1 km depth, there is a pronounced, 2-km-wide, 1-km-high high-velocity (5000 m/s) anomaly (Fig. 5). This anomaly lies west of the active trace of the HF and has nearly vertical edges, consistent with strike-slip structural style. The anomaly may represent a relatively uplifted block (a horst of sorts) between two steeply-dipping strike-slip faults. This anomaly coincides with an interpreted serpentinite body (Ponce et al., 2003).

- S-wave velocity models, developed using MASW analysis, show low-velocity anomalies that coincide with known faults. Such anomalies are observed along all three of the 20-m-spaced arrays deployed over the major fault zones (Fig. 7b, c, d). This is not surprising because the topography patterns, the near-penetrative brittle-plastic deformation throughout most of the SLB, and the likelihood that the major faults within the greater HFZ will have splays and may 'feather' at the surface is consistent this type of faulting, as inferred from the MASW models.

7.0 CONCLUSION

The original aim of this study was to conduct one or two medium-scale (0.5-1 km) seismic surveys across the San Leandro Block near the cities of San Leandro and Hayward, California. Our initial goal was to understand the three-dimensional geometry and connectivity of the Hayward and Chabot faults. Our actual survey that was acquired in the Fall of 2016 was much larger, extending 15 km in length and crossing a large portion of the greater Hayward Fault Zone. The high quality and resolution of the datasets allow us to develop P-wave tomographic velocity models that show anomalies beneath the East Bay plain and areas of localized low P-wave velocities to the northeast. Anomalies seen on our 2-D MASW shear-wave velocity models correspond well with mapped faults and infer additional unmapped faults. We are confident that further exploration of the datasets will provide significant new insights into the tectonic structures of the East Bay plain and hills and the Hayward Fault zone.

8.0 ACKNOWLEDGEMENTS

This study was funded in part by the USGS Earthquake Hazard Program Award G16AP00096. We would like to thank the East Bay Regional Park District, the East Bay Municipal Utility District, Alameda County, City of San Leandro, San Lorenzo Unified School District, City of Oakland, Alameda County Flood Control, Hayward Area Recreation District, Seneca School, Mills College, Sequoyah Golf Course, Redwood Canyon Golf Course, and the AMMA Center. We would like to thank the following individuals:

- USGS personnel, interns, and volunteers: Carolyn Steiben, Joey Mason, Keith Galvin, Blathnaid McKevitt, Ryota Kiuchi, Dan Langermann, William Seelig, Devin Minnich, Edward Zhang, James Bamford, and Jacyn Schmidt.
- CSUEB graduate and undergraduate students: Chris Dobel, Nathan Suits, David Saucedo-Green, Jennie Baharamian, Bobby Savoy, Brenda Delgadillo, Nick Sadler, Elin Svedberg, Damon Quinby, Adolfo Perez, Tiara Richard, and Natalie Arreaga.
- Other volunteers and friends of EB3D: Connie Ing, Brent Johnson, Dan Hollis, and Ryan Fay.

Enormous thanks especially to Murray Nicolson for generously hosting our staging area during deployment. Thanks also to Bob Fusinati and the 'Mayor of Cull Canyon' (Jim Panico) for access to their properties. Thank you so much to Pamela Beitz for guiding us through the East Bay Regional Parks permitting processes. In addition, we would like to thank Luke Blair of the USGS for help with GIS during the Summer of 2016 and the folks at CSUEB facilities management for helping with logistics.

9.0 REFERENCES

Abimbola, A. O., Strayer, L. M., McEvilly, A. T., Chan, J. H., 2016, Ground-Truth on The CSUEB Campus: Results From Integrating Geophysical, Geological and Geospatial Methods and Fault Trench Studies, Seismological Society of America Annual Meeting, Reno, 2016, SRL Vol. 87, No. 2B

Borcherdt, R.D., 1970, Effects of local geology on ground motion near San Francisco Bay, Bull. Seism. Soc. Am, 60, 29-61.

Borcherdt, R.D. and Glassmoyer, G., 1992, On the characteristics of local geology and their influence on ground motions generated by the Loma Prieta earthquake in the San Francisco Bay region, California, Bull. Seism. Soc. Am., 82, 603-641.

Borcherdt, R.D., 2002, Empirical evidence for site coefficients in building code provisions, Earthquake Spectra, v. 18, no. 2, p. 189-217.

Bürgmann, R., Schmidt, D., Nadeau, R.M., d'Alessio, M., Fielding, E., Manaker, D., McEvilly, T.V., and Murray, M.H., 2000, Earthquake potential along the northern Hayward Fault, California, Science, Vol. 289, 1178–1182

Byerlee, James D., 1978, Friction of rocks, Pure and Applied Geophysics, No. 116, pp. 615–626.

Catchings, R. D., Goldman, M. R., Chan, J. H., Sickler, R. R., Strayer, L. M., Boatwright, J., Criley, C. J., 2017, Basin-Wide Vp, Vs, Vp/Vs, And Poisson's Ratios Of The Napa Valley, California, Seismological Society of America Annual Meeting, Denver, 2017, SRL Vol. 88, No. 2B

Catchings, R.D., L. M. Strayer, M. R. Goldman, C. J. Criley, S. Garcia, R. R. Sickler, M. K. Catchings, J. Chan, L. C. Gordon, S. Haefner, J. L. Blair, G. Gandhok, & M. R. Johnson, 2015, 2013 East Bay Seismic Experiment (EBSE): implosion data, Hayward, California. http://dx.doi.org/10.5066/F7BR8Q75

Catchings, R.D., Strayer, L.M., Goldman, M.R., Criley, C.J., Garcia, S.H., Sickler, R.R., Catchings, M.K., Chan, J.H., Gordon, L., Haefner, S., Blair, L., Gandhok, G., and Johnson, M., 2015, 2013 East Bay Seismic Experiment (EBSE) - Implosion Data, Hayward, Calif: U.S. Geological Survey data release, http://dx.doi.org/10.5066/F7BR8Q75, https://pubs.er.usgs.gov/publication/70144317.

Catchings, R.D., M.R. Goldman, M.J. Rymer, 2007, Multi-Methods High-Resolution Seismic Imaging of Active Fault Zones. *Eos Trans. AGU, 88*(52), Fall Meet. Suppl., Abstract NS23A-06.

Catchings, R.D., D.S. Powars, G.S. Gohn, & M.R. Goldman, 2006a, High-Resolution Seismic-Reflection Image of the Chesapeake Bay Impact Structure, NASA Langley Research Center, Hampton, Virginia, *in* Studies of the Chesapeake Bay Impact Structure— The USGS-NASA Langley Corehole, Hampton, Virginia, and Related Coreholes and Geophysical Surveys, J.W. Horton, Jr., D.S. Powars, & G.S. Gohn Editors.

Catchings, R.D., Borchers, J.W., Goldman, M.R., Gandhok, G., Ponce, D.A., and Steedman, C.E., 2006b, Subsurface structure of the East Bay Plain Ground-Water Basin: San Francisco Bay to the Hayward Fault, Alameda County, California, United States Geological Survey Open-File Report 2006-1084 2006.

Dibblee Jr., T.W., 1980, Preliminary geologic map of the Hayward Quadrangle, Alameda and Contra Costa counties, California: Open-File Report USGS Numbered Series 80-540, http://pubs.er.usgs.gov/publication/ofr80540.

Fossen, H., 2010, Structural Geology, Cambridge University Press.

Graymer, R.W., 2000, Geologic map and map database of the Oakland Metropolitan area, Alameda, Contra Costa, and San Francisco Counties, California, U.S. Geological Survey, Miscellaneous Field Studies, MF-2343, version 1, scale 1:50,000.
Graymer, R.W., Jones, D.L., and Brabb, E.E., 1995, Geologic map of the Hayward Fault zone:U.S. Geological Survey Open File Report 95-597, scale 1:50,000.
Graymer, R. W., Jones, D.L. and E. E. Brabb, 1995, Is there more Quaternary displacement on the Chanobt Faultthan on the Hayward Fault, American Association of Petroleum Geologists Bulletin, No. 79, pg. 585.
Hayashi, K., and Suzuki, H., 2004, CMP cross-correlation analysis of multi-channel surface-wave data: Exploration Geophysics, v. 35, p. 7-13.
Hole, J.A. 1992, Nonlinear high-resolution three-dimensional seismic travel time tomography. J. Geophys. Res., 97, pp. 6553-6562.
Holzer, T.L., 1994, Loma Prieta damage largely attributed to enhanced ground shaking, EOS Trans. Am. Geophys. Union, v. 75, no. 26, p. 299-301.
Holtzer, T.L., Padovani, A.C., Bennett, M.J., Noce, T.E., Tinsley, J.C., 2005, Mapping NEHRP Vs30 site classes, Earthquake Spectra, v. 21, no. 2, p. 1-18.
Li, Y.G., and Vidale, J.E., 1996, Low-velocity fault-zone guided waves: Numerical investigations of trapping efficiency, Bulletin of the Seismological Society of America, Vol. 86, pp. 371-378.
Li, Y.G., and Leary, P. C., 1990, Fault zone trapped seismic waves, Bulletin of the Seismological Society of America, Vol. 80, pp. 1245–1271.
Lienkaemper, J.J., Revised 2008, Digital database of recently active traces of the Hayward Fault, California, United States Geological Survey, Map DS-177.
Maffei, J. & Knudsen, K., et al., 2010, The coming bay area earthquake-2010 update of scenario for a magnitude 7.0 earthquake on the Hayward Fault, United States Geological Survey Technical Report, 08HQAG0116.
McEvilly, A. T., Strayer, L. M., Chan, J. H., Abimbola, A., 2017, High-Resolution Tomography Of Vp, Vs, Vp/Vs, And Poisson's Ratios Of Quaternary-Active Chabot Fault Of The Hayward Fault Zone, Seismological Society of America Annual Meeting, Denver, 2017, SRL Vol. 88, No. 2B.
McEvilly, A. T., Strayer, L. M., Abimbola, A., Chan, J. H., 2016, Mapping The Geometry Of The San Leandro Block, Hayward Fault Zone Using Geologic And Geophysical Methods; California State University, East Bay Campus, Seismological Society of America Annual Meeting, Reno, 2016, SRL Vol. 87, No. 2B.
Midland Valley, Move2017.2 software, http://www.mve.com
Mount, V., and Suppe, J., 1987, State of stress near the San Andreas fault: Implications for wrench tectonics: Geology, Vol. 115, pp. 1143–1146.
Nazarian, S., Stokoe, K., Sheu, J., and Wilson, C., 1986, Near surface profiling of geotechnical sites by surface wave method, *in* SEG Technical Program Expanded Abstracts 1986, Society of Exploration Geophysicists, SEG Technical Program Expanded Abstracts, p. 126-129, https://doi.org/10.1190/1.1893189.
Park, C., Miller, R., Xia, J., and Ivanov, J., 2000, Multichannel analysis of surface waves (MASW)—active and passive methods: The Leading Edge, v. 26, p. 60–64, doi: 10.1190/1.2431832.
Park, C., 2005, Shear Wave Velocity (Vs) Profiling by Surface Wave (MASW) Method, *in* Symposium on the Application of Geophysics to Engineering and Environmental Problems

2005, Environment and Engineering Geophysical Society, Symposium on the Application of Geophysics to Engineering and Environmental Problems, p. 581–582, https://doi.org/10.4133/1.2923509 (accessed August 2017).

Ponce, D.A., Hildenbrand T. G., and Jachens R. C., 2003, Gravity and Magnetic Expression of the San Leandro Gabbro with Implications for the Geometry and Evolution of the Hayward Fault Zone, Northern California, Bulletin of the Seismological Society of America, Vol. 93, No. 1, pp. 14–26.

Pujol, J., 2003, Elastic Wave Propagation and Generation in Seismology, Cambridge University Press, United Kingdom.

Radbruch-Hall, D.H., 1974, Map showing recently active breaks along the Hayward Fault zone and the southern part of the Calaveras fault zone, California: U.S. Geological Survey Miscellaneous Investigations Series Map I-813, scale 1:24,000.

*Richardson, I. S., Strayer, L. M., Chan, J. H., McEvilly, A. T., 2017, Shallow Vs Structure Of Subsidiary Faults In The Hayward Fault Zone Inferred From Multichannel Analysis Of Surface Waves (MASW), Seismological Society of America Annual Meeting, Denver, 2017, SRL Vol. 88, No. 2B

Rubin, R.S., 2011, California Geological Survey Fault Evaluation Report Fer-255 Ashland Fault, Alameda County, California gmw.conservation.ca.gov/shp/EZRIM/Reports/.../FER_255_ Report _20110621.pdf

Science Channel, 2017, *Secrets of the Underground – California's Hidden Doomsday*, https://www.sciencechannel.com/tv-shows/secrets-of-the-underground/full-episodes/californias-hidden-doomsday

Toppozada, T. R., Branum, D. M., Reichle, M. S. and Hallstrom, C. L., 2002, San Andreas fault zone, California: M≥ 5.5 earthquake history. Bulletin of the Seismological Society of America Vol. 92, 2555–2601.

Strayer, L. M., Catchings, R. D, Goldman, M. R, Chan, J. H ., Sickler, R. R., McEvilly, A. T., Richardson, I. S, 2016, The 2016 East Bay Seismic Investigation: Seismic Tomography Imaging Across The Hayward Fault Zone Near San Leandro, California, American Geophysical Union Annual Fall Meeting, San Francisco, 2016

Strayer, L. M., Catchings, R. D, McEvilly, A. T., Chan, J. H., Goldman, M. R., Criley, C. J., Richardson, I. S., Sickler, R. R., 2017, The 2016 East Bay Seismic Investigation: Seismic Tomography Imaging Across The Hayward Fault Zone Near San Leandro, California, Seismological Society of America Annual Meeting, Denver, 2017, SRL Vol. 88, No. 2B

Waldhauser, F. & Ellsworth, W. L., 2002, Fault structure and mechanics of the Hayward Fault, California, from double-difference earthquake locations, Journal of Geophysical Research: Solid Earth, Vol. 107, ESE–3

Wakabayashi, J. 1999, Distribution of displacement on and evolution of a young transform fault system: the northern San Andreas fault system, California, Tectonics 18, 1245–1274.

Wakabayashi, J., 2007, Stepovers that migrate with respect to affected deposits: field characteristics and speculation on some details of their evolution, *in* Tectonics of Strike-Slip Restraining and Releasing Bends, Cunningham, W. D. & Mann, P. (eds). Geological Society, London, Special Publications, 290, 169–188.

Working Group on California Earthquake Probabilities, 2003, Earthquake probabilities in the San Francisco Bay region: 2002-2031, United States Geological Survey Open-File Report 03-214.

Xia, J., Miller, R., Park, C., and Ivanov, J., 2000b, Construction of 2 D Vertical Shear Wave Velocity Field by the Multichannel Analysis of Surface Wave Technique, *in* Symposium on the Application of Geophysics to Engineering and Environmental Problems 2000, Environment and Engineering Geophysical Society, Symposium on the Application of Geophysics to Engineering and Environmental Problems, p. 1197–1206, https://doi.org/10.4133/1.2922726 (accessed August 2017).

Wills, C.J., Gutierrez, C.I., Perez, F.G., Branum, D.M., 2015, A next generation Vs30 map for California based on geology and topography, Bulletin of the Seismological Society of America, v. 105, no. 6, p. 3083-3091.

Yu, E., and Segall, P., 1996, Slip in the 1868 Hayward earthquake from the analysis of historical triangulation data: Journal Geophysical Research, Vol. 101, No. 16, pp. 101–16,118.

10.0 FIGURES

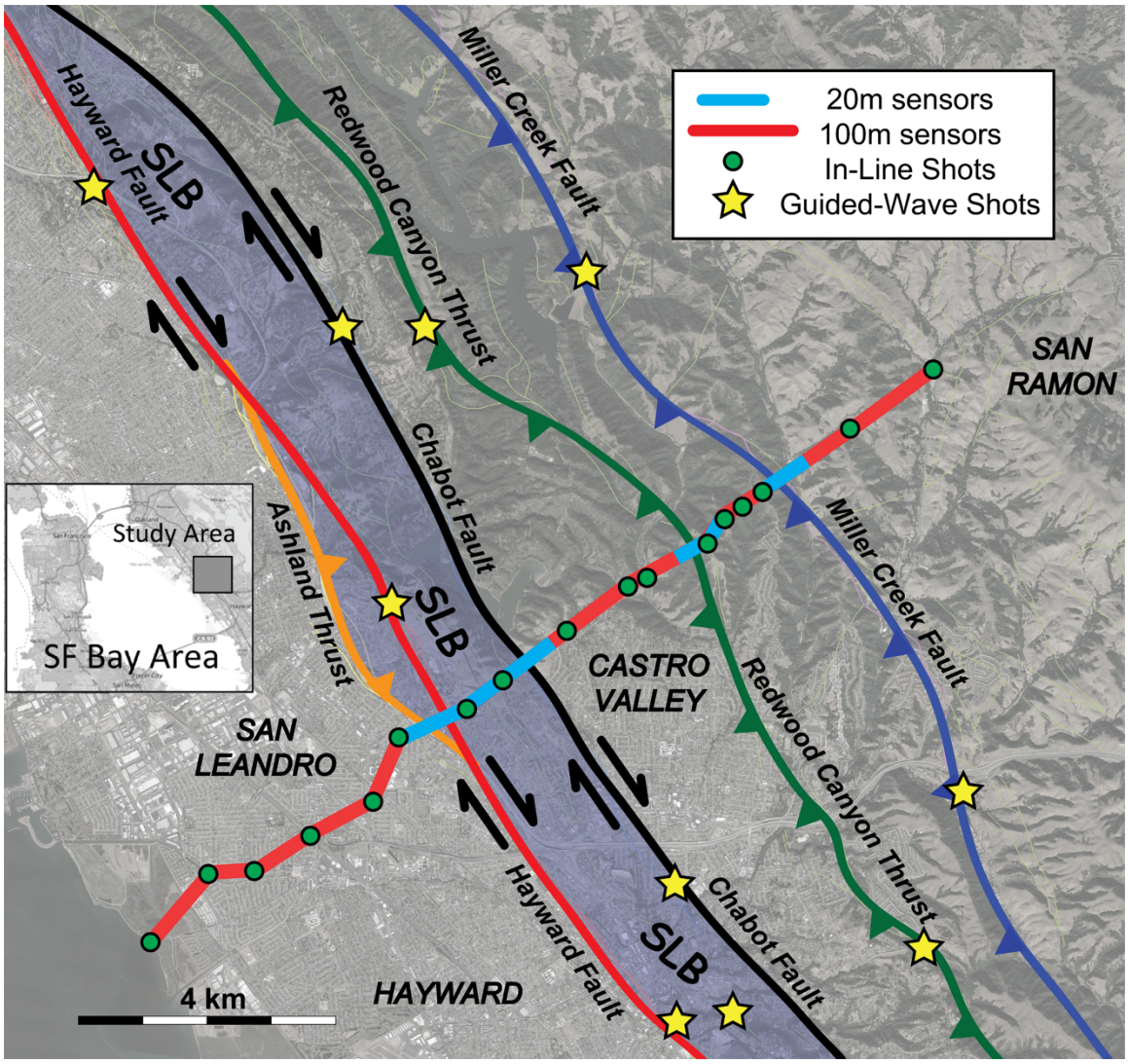

Figure 1. Elements of the East Bay Seismic Investigation (EBSI-16)
Map of the study area, the San Leandro block (SLB), and major faults of the greater Hayward Fault zone. The trace of the seismic array (red line) strikes 054°, with two-component (horizontal and vertical) sensors deployed at 100-m intervals and one-component (vertical) sensors deployed at 20-m intervals (blue) where it crosses major faults. Green circles represent in-line, buried explosive shot-points, and yellow stars identify guided-wave shot-points.

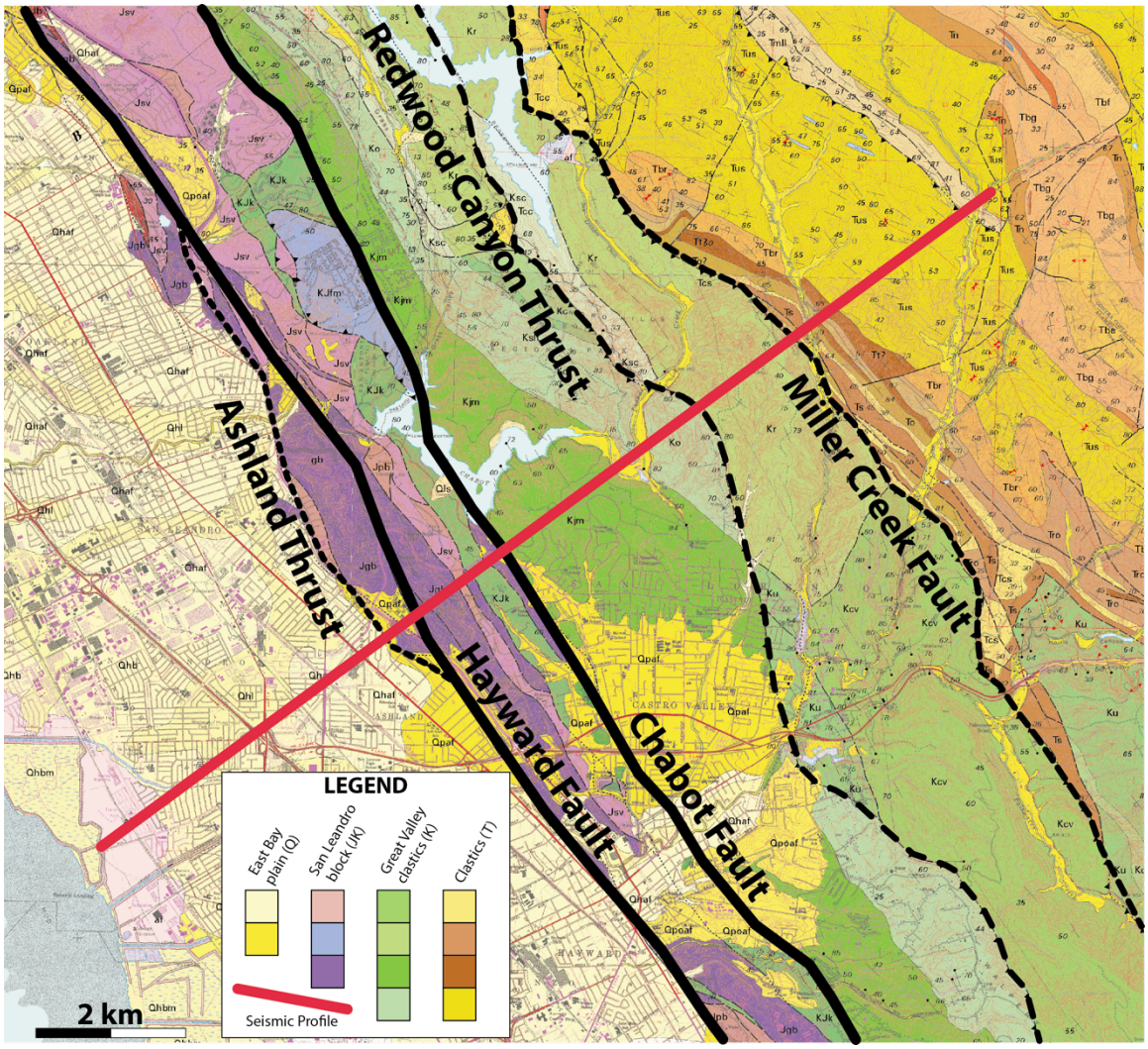

Figure 2. Geology and lithotectonic elements of the EBSI-16 study area
Geologic map (Graymer, 2000) showing the EBSI-16 study area, the major faults of the greater Hayward Fault zone, and the location of the resultant seismic profiles. Faults separate important lithotectonic domains.

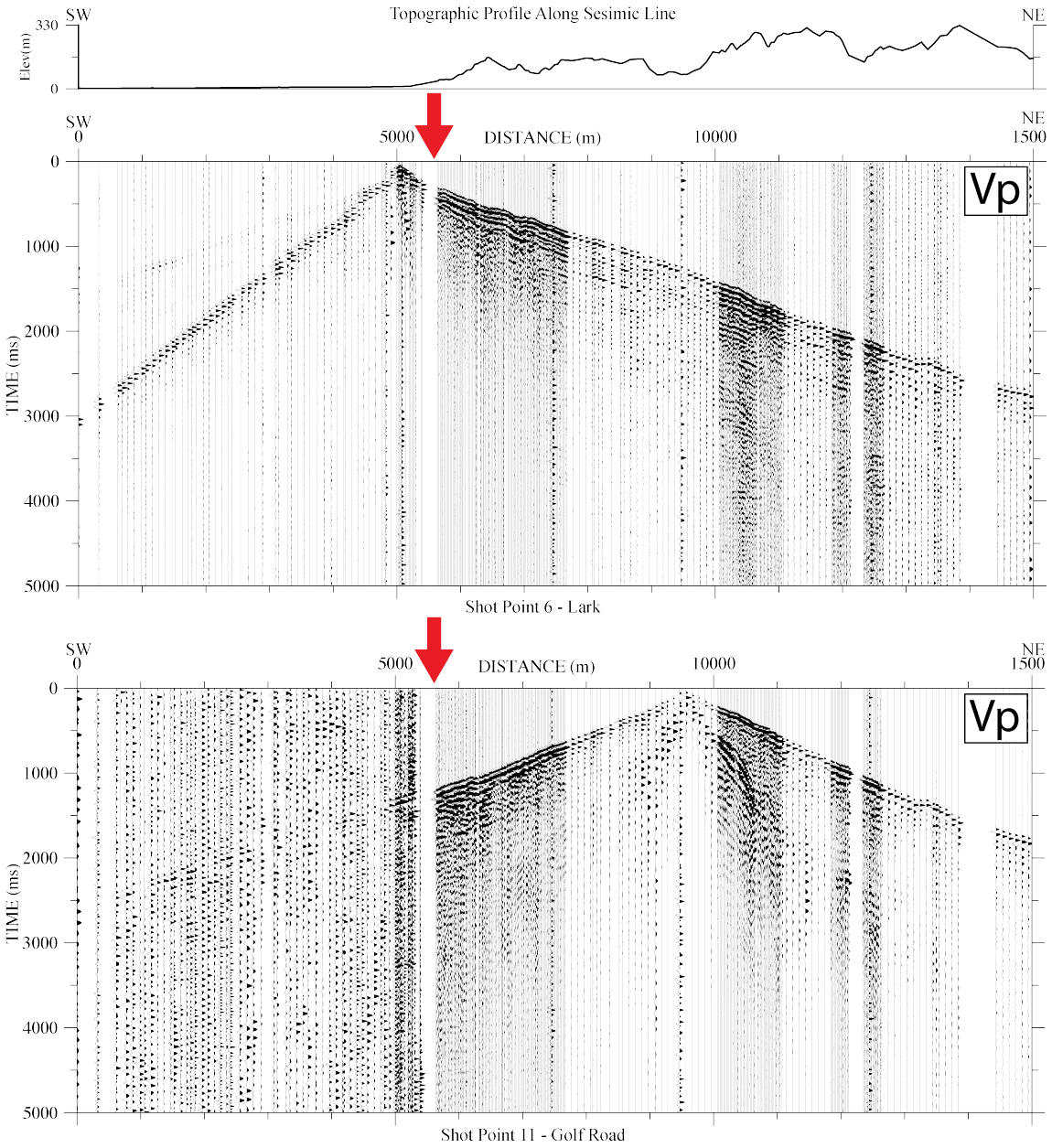

Figure 3. Example of P-Wave Shot Gathers
Two example P-wave shot gathers located on either side of the active trace of the Hayward Fault (~5600 m). Sensor spacing was 100 m, with 20-m spacing across major faults of the HFZ (dense spacing). Gaps in sensor coverage result from lack of access (I-580) and permission issues. The bottom figure suggests the Hayward Fault (red arrow) acts a barrier to P-wave propagation to the southwest

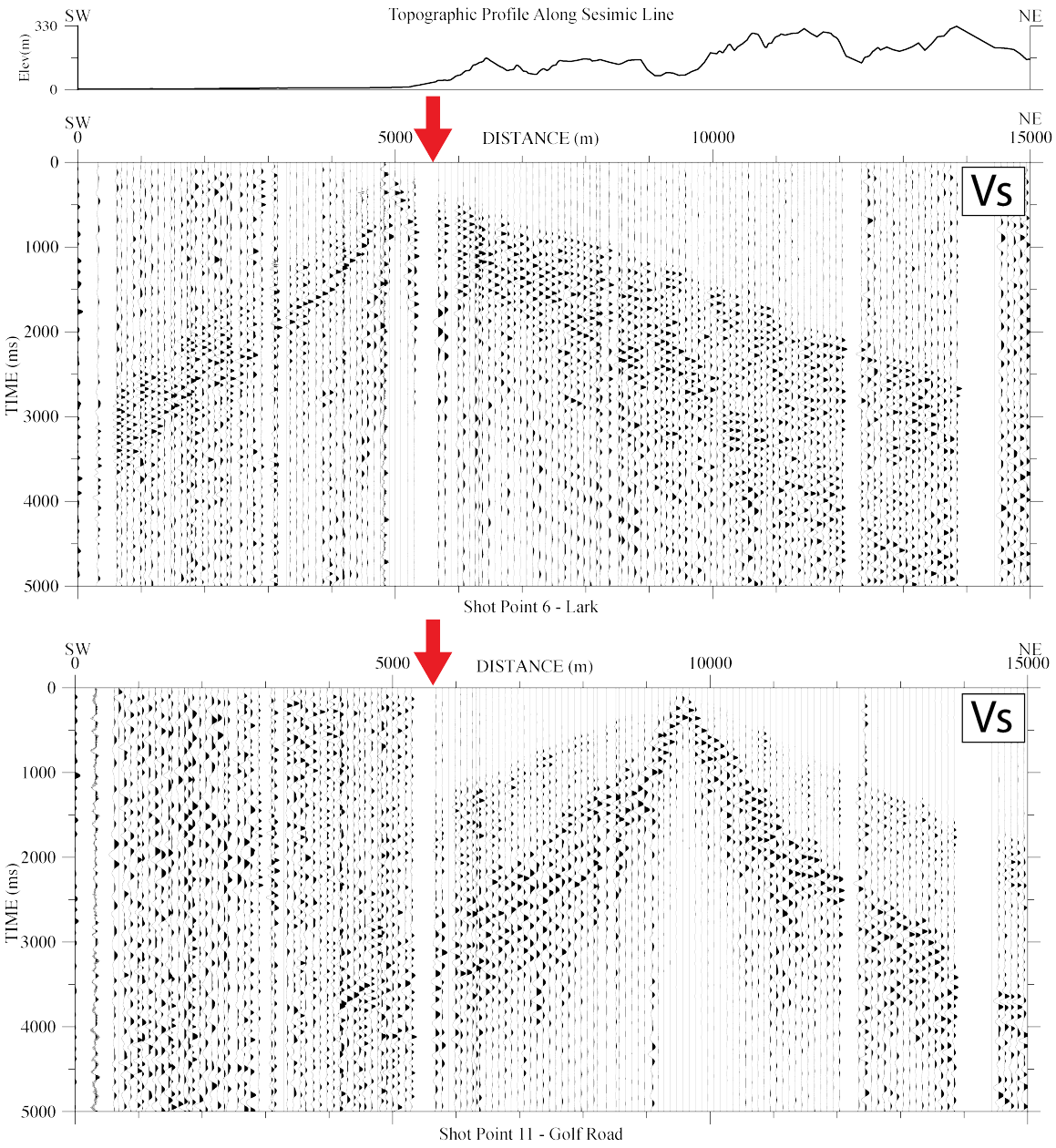

Figure 4. Example of S-Wave Shot Gathers
Two examples of S-wave data from either side of the active trace of the Hayward Fault (~5600 m). Sensor spacing is 100 m. Gaps in sensor coverage are the result of access (I-580) and permission issues. The Hayward Fault (red arrow) acts a barrier to S-wave propagation to the southwest in the bottom figure.

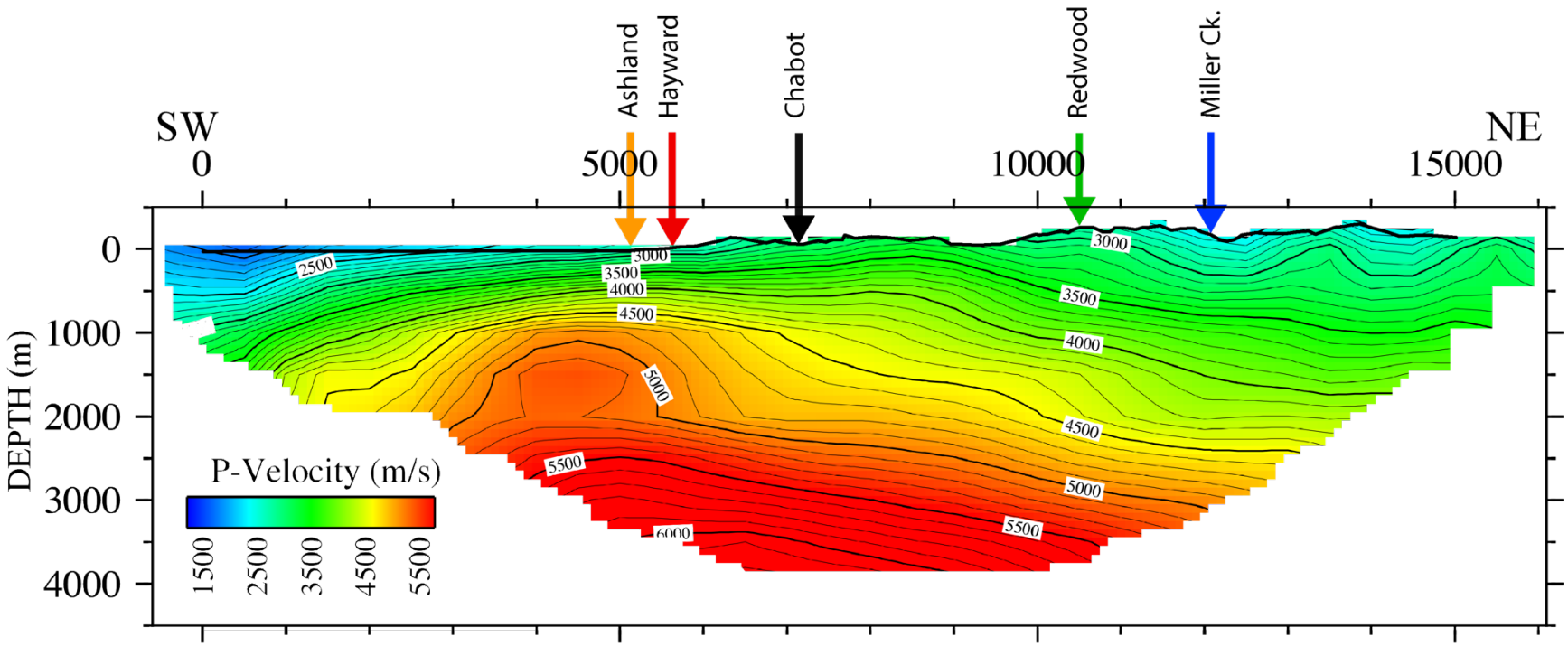

Figure 5. P-wave Refraction Tomography
P-wave velocity model across the entire East Bay plain and a large part of the East Bay hills, including the San Leandro block. Arrows point to the approximate locations of faults. Lowest P-wave velocities are in the southwest at the San Leandro tidal marsh. High velocity P-wave structure appears at a depth of 1500 m, just west of the Ashland thrust.

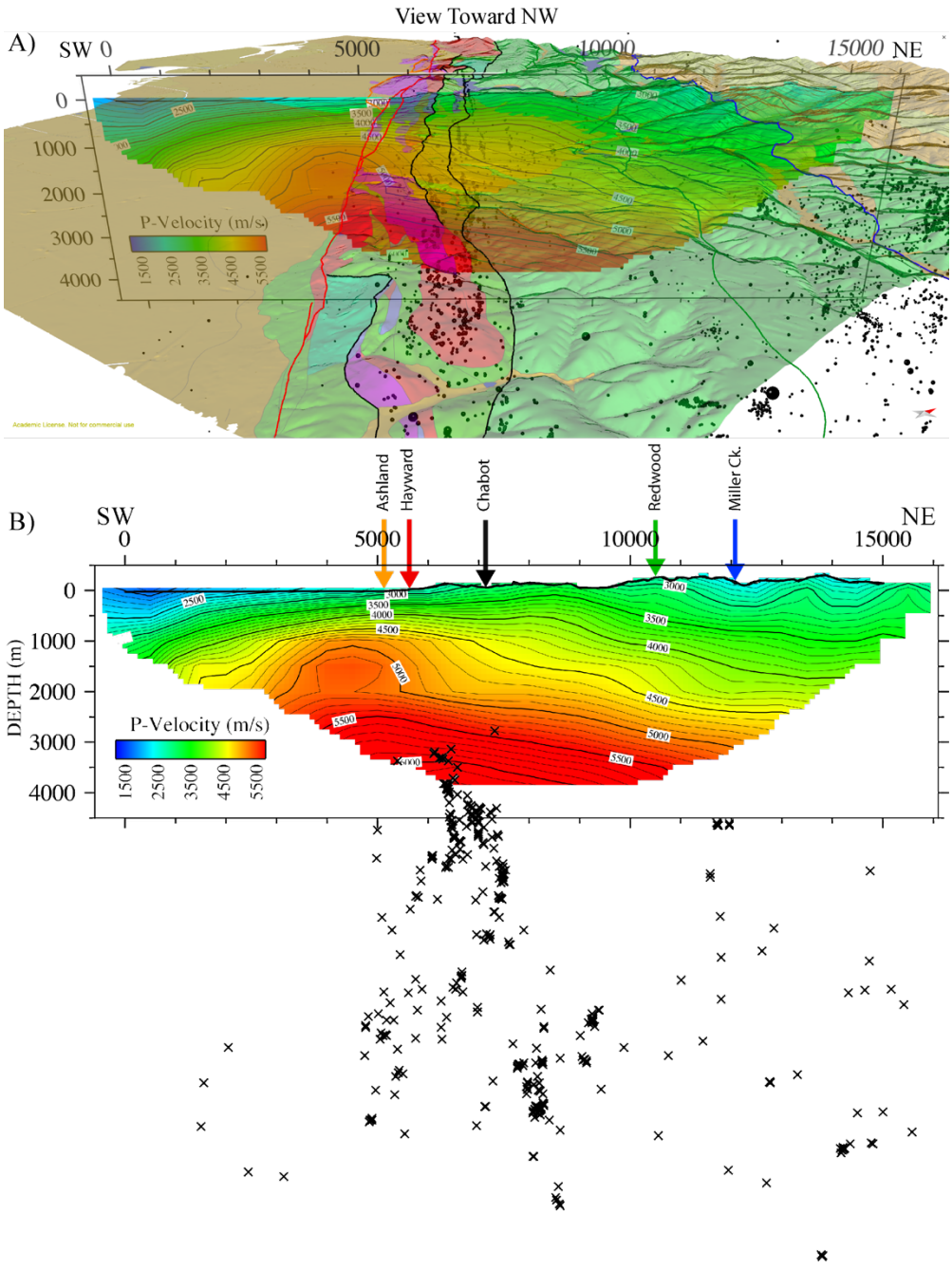

Figure 6. P-wave Refraction Tomography Model and Relocated Earthquakes
A) Preliminary P-wave velocity model within a 3D context, showing topography, geology, faults, and relocated seismicity. **B)** P-wave velocity model shown with relocated earthquakes superimposed, with a 4-km-wide swath of seismicity projected onto the seismic profile.

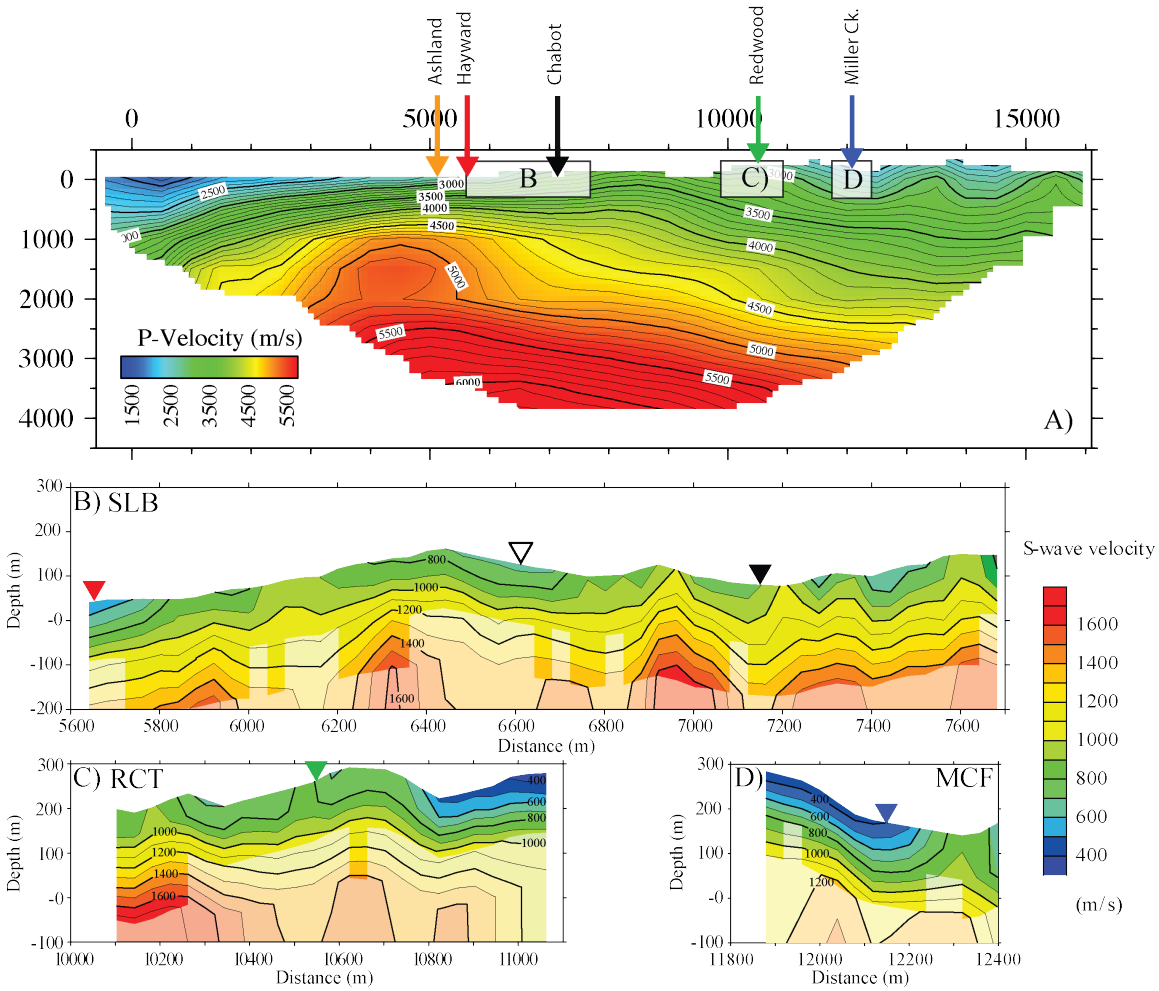

Figure 7. P-wave Tomography and MASW 2-D Shear-Wave Velocity Models
A) P-wave velocity model with locations of three MASW velocity models: models B, C, and D. **B)** MASW velocity model across the San Leandro block, with the locations of the active trace of the Hayward Fault (red triangle), the West Chabot Fault (white triangle), and the East Chabot Fault (black triangles). **C)** MASW velocity model across the Redwood Canyon Thrust Fault, with the mapped locations of the fault (green triangle). **D)** MASW velocity model across the Miller Creek Fault, with the fault location (blue triangle).